

Phase Contrast Imaging with Coded Apertures Using Laboratory-Based X-ray Sources

K. Ignatyev, P. R. T. Munro, R. D. Speller, and A. Olivo

Citation: [AIP Conference Proceedings](#) **1365**, 254 (2011);

View online: <https://doi.org/10.1063/1.3625352>

View Table of Contents: <http://aip.scitation.org/toc/apc/1365/1>

Published by the [American Institute of Physics](#)

Articles you may be interested in

[A coded-aperture technique allowing x-ray phase contrast imaging with conventional sources](#)

Applied Physics Letters **91**, 074106 (2007); 10.1063/1.2772193

[Differential x-ray phase contrast imaging using a shearing interferometer](#)

Applied Physics Letters **81**, 3287 (2002); 10.1063/1.1516611

Phase Contrast Imaging with Coded Apertures Using Laboratory-Based X-ray Sources

K. Ignatyev, P. R. T. Munro, R. D. Speller, and A. Olivo

Department of Medical Physics and Bioengineering, University College London, London, UK

Abstract. X-ray phase contrast imaging is a powerful technique that allows detection of changes in the phase of x-ray wavefronts as they pass through a sample. As a result, details not visible in conventional x-ray absorption imaging can be detected. Until recently the majority of applications of phase contrast imaging were at synchrotron facilities due to the availability of their high flux and coherence; however, a number of techniques have appeared recently that allow phase contrast imaging to be performed using laboratory sources. Here we describe a phase contrast imaging technique, developed at University College London, that uses two coded apertures. The x-ray beam is shaped by the pre-sample aperture, and small deviations in the x-ray propagation direction are detected with the help of the detector aperture. In contrast with other methods, it has a much more relaxed requirement for the source size (it works with source sizes up to 100 μm). A working prototype coded-aperture system has been built. An x-ray detector with directly deposited columnar CsI has been used to minimize signal spill-over into neighboring pixels. Phase contrast images obtained with the system have demonstrated its effectiveness for imaging low-absorption materials.

Keywords: Phase contrast, coded apertures, x-ray imaging.

PACS: 07.85.Fv

INTRODUCTION

Recently there has been a lot of interest in the development of x-ray phase contrast imaging techniques and their application in various fields such as materials science and biology [1, 2]. The main advantage of phase contrast imaging compared to conventional x-ray imaging is its increased sensitivity to small changes in the sample density and composition. Traditionally, before the advent of phase contrast methods, recorded image contrast was mostly due to differences in absorption paths for different x-rays. Absorption imaging cannot resolve small changes in sample density and composition. The index of refraction can be written as

$$n = 1 - \delta - i\beta, \quad (1)$$

where δ is the deviation of the real part of the index of refraction from unity, and β is the imaginary part of the index of refraction and is proportional to the linear attenuation coefficient. The advantage of x-ray phase contrast imaging (XPCi) is that it allows measuring changes in δ , which is about three orders of magnitude larger than β for light materials at typical x-ray energies used in imaging.

X-ray phase contrast imaging really took off with the advent of third-generation synchrotron sources. The high spatial coherence of synchrotron x-rays allows the phase contrast to be obtained without employing any optical elements between a sample and a detector in so-called in-line phase contrast imaging [3]. Other well-known phase contrast techniques are diffraction-enhanced imaging (DEI), which uses analyzer crystals placed after the sample [4], and the Bonse-Hart interferometry method [5]. Both techniques allow quantitative information about the change of phase in the sample to be obtained; this is straightforward with the interferometry method but requires multiple images with DEI. Quantitative information can also be reconstructed with in-line holography by reconstructing images recorded at several sample-detector distances [6].

Stunning synchrotron phase contrast results have been demonstrated recently; for example, it became possible to perform *in vivo* studies of the processes associated with the breathing of insects [2]. It would be a great breakthrough for medical imaging and other modalities if phase contrast imaging methods could be transferred from the synchrotron environment into real-world applications. Limited efforts have been made to bring patients to the

synchrotron [7], and several medical beamlines are currently being constructed; however, the availability will still be very limited into the near future, thus preventing widespread applications in radiology.

There are currently active efforts to use phase contrast imaging in the laboratory setting. It was shown some time ago [8] that phase contrast can be obtained with laboratory sources. One of these promising methods is a technique that uses Talbot interferometry with several gratings placed between the sample and detector [9]. A third grating placed after the x-ray source must be employed in the laboratory version of the technique to create an array of individually coherent sources. An alternative method to obtain individual coherent sources is to cut grooves in the anode target of the x-ray source [10].

Our group recently proposed and described a different method to perform phase contrast imaging, using coded apertures, that does not rely on the wave interference [11]. This, in turn, relaxes minimal conditions placed on the temporal coherence, energy, and size of the x-ray source, and makes the technique achievable for medical, security, and industrial applications using existing commercial sources. As an added advantage, Talbot distances do not have to be satisfied. The technique is based on the concept of pixel edge illumination: by blocking part of the detector pixel, it becomes sensitive to small changes in the x-ray propagation direction resulting from refraction in a sample. Effectively it becomes possible to measure refraction in the sample, which can be thought of as a manifestation of phase contrast in geometrical optic terms.

The method uses two absorption apertures; however, these play a completely different role than the ones in a grating interferometer. The first aperture, positioned directly in front of a sample, splits the beam into a multitude of individual beams. After interaction with a sample, these beams impact on the second aperture—located in front of the detector—which blocks part of each pixel. Since no interference is involved, the grating period can be made much larger, with the only requirement being that it matches the detector pixel dimensions. The apertures can consist of line gratings for sensitivity to phase changes in one dimension, or they can be made with periodic “L”-shaped gratings for two-dimensional phase imaging.

MATERIALS AND METHODS

The phase contrast imaging setup, as shown in Fig. 1(a), consists of a commercial rotating tungsten anode x-ray tube, two sets of coded masks or apertures, a sample holder, and a detector. The tube focal spot size of 50 μm was measured by imaging an absorbing thin copper plate edge at several distances from the source. Images were recorded at several tube voltages varying from 40 kVp to 100 kVp, and the tube current at all voltages was 1 mA. No x-ray filtering was used except for a 1-mm aluminum exit window, and the full polychromatic spectrum was used. Gold was selected as the absorbing material for the masks. Several mask designs were used for the imaging; the ones with the largest field of view had dimensions of 6 \times 6 cm for the detector mask and 4.8 \times 4.8 cm for the pre-sample mask (dimensions vary due to cone beam magnification). Figure 1(b) shows a typical mask pattern. The manufacturing process used to create the masks can easily scale them up to 30 \times 30 cm; they have to be tiled if larger fields of view are needed. One set of masks was non-line-skipping, that is, every detector pixel column was illuminated; and the other set consisted of line-skipping masks so that every other detector column was shadowed. The reason for this was to explore the effect of scintillator photon spread and charge sharing in adjacent pixels, which can smear out the phase contrast in the resulting image. It was observed that the non-line-skipping masks also gave good phase contrast. Each mask was mounted on a high-precision translation-rotation motor stack allowing movement with four degrees of freedom: two translations and two rotations for mask alignment. These are also used to adjust the experimental conditions. First, the detector mask is aligned with respect to the detector pixel columns, and then the pre-sample mask is aligned with the detector mask. By translating the pre-sample mask in the transverse direction it is possible to change the sensitivity of the system to small refraction angles, thus making the system flexible to image different types of samples. The analogue of this in diffraction-enhanced imaging would be the detuning of the analyzer crystal.

The detector consisted of a 2 K \times 2 K CMOS pixel array with pixel size of 50 μm and a directly deposited columnar-grown CsI scintillator to reduce the lateral spread of photons. Typical exposure time with tube current of 1 mA was one minute for one sample position. It may be advantageous in some cases to take several exposures at different transverse sample positions in order to increase the spatial resolution of the system. The reason for this is that the resolution of the system is not solely determined by the detector pixel size or scintillator parameters, but also by the relative displacement of the two masks. By only illuminating a small part of the detector pixel it is possible to obtain images at a resolution higher than would be achievable in a normal imaging setup with the same detector. The down side to it is that parts of the sample remain shadowed by the mask; information from these areas can be retrieved by recording images at several sample positions and recombining them (“stitching”) in a single image.

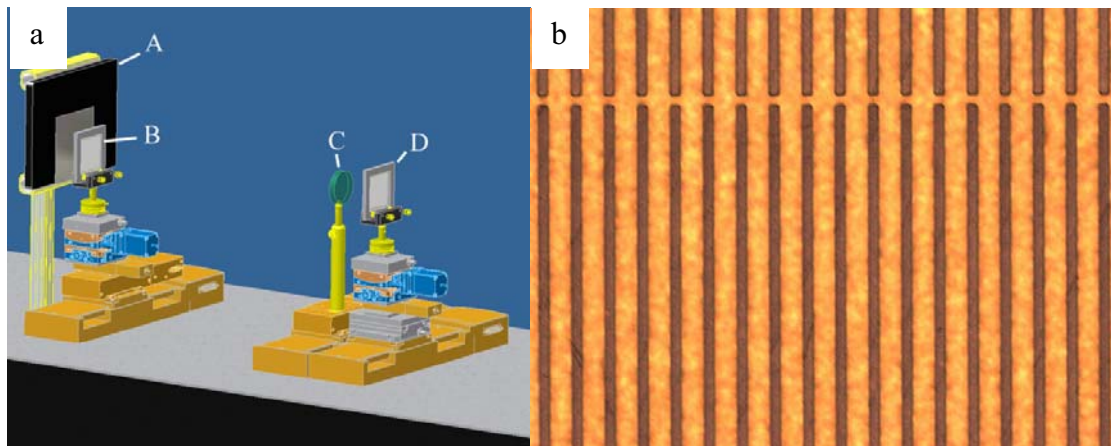


FIGURE 1. (a) Schematic layout of the XPCi experimental setup. The x-ray source is not shown. From left to right are detector (A), detector aperture (B), sample (C), and sample aperture (D). The x-ray propagation direction is from right to left. (b) Optical micrograph of the detector aperture used in the experiment. Brighter areas represent vertical lines 70- μm -wide, 200- μm -thick gold columns that block x-rays; darker areas are transparent for x-rays. Grid period is 98 μm . The horizontal gold line at the top of the image is for structural support of the gold lines.

RESULTS

Figure 2 shows the image of a sample recorded with the coded apertures. The sample consisted of several vertical 75- μm aluminum wires (one on the right side of the image and one on the left) and one 300- μm vertical polyethylene fiber in the center. All wires clearly show edge enhancement associated with phase contrast and are completely invisible in the conventional absorption images recorded with the same x-ray statistics but without coded apertures. The image in Fig. 2 was constructed from images recorded at five sample positions to increase the resolution by interleaving individual image columns; however, even individual images recorded at a single sample position show sufficient contrast at the parts of the sample that are illuminated by the x-ray beam. The image in Fig. 2 was recorded at a tube voltage of 60 kVp; however, more data were recorded at several tube voltages ranging from 40 kVp to 100 kVp, and even at 100 kVp there was still noticeable image contrast. In addition to x-ray energy, another parameter that affects imaging conditions is the percentage of illumination of the detector pixels. By shifting the masks in a direction normal to the beam and mask aperture lines, it is possible to change the number of photons reaching the detector as well as select a specific angular range of the refracted beam. It is possible to perform dark-field imaging by completely blocking direct beam and only detecting the refracted portion of it. Of course there is a trade-off between the sensitivity to phase contrast and signal-to-noise ratio, which has to be optimized according to the specific imaging situation.

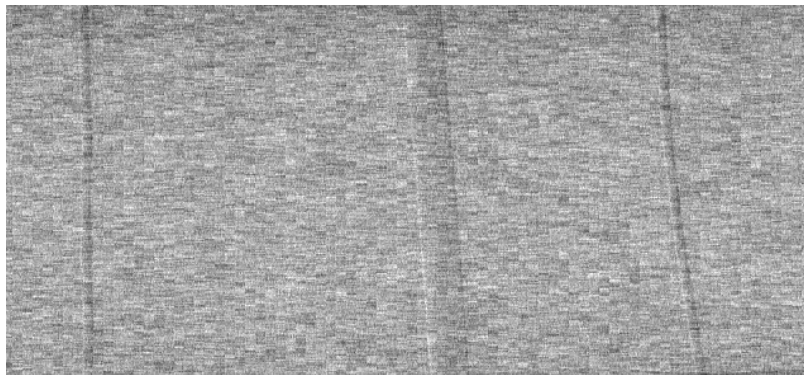


FIGURE 2. X-ray phase contrast image obtained with coded apertures at 60-kVp tube voltage.

A typical measured wire profile is shown in Fig. 3 with superimposed profile calculated considering refraction in the weakly absorbing wire using the geometrical optics approach [12]. At the current stage of development phase contrast imaging with coded apertures provides qualitative enhancement of the contrast otherwise not seen with absorption. There is a potential of using it to obtain quantitative information, that is, reconstructing a phase changed by the sample, and it is the subject of future work in this area.

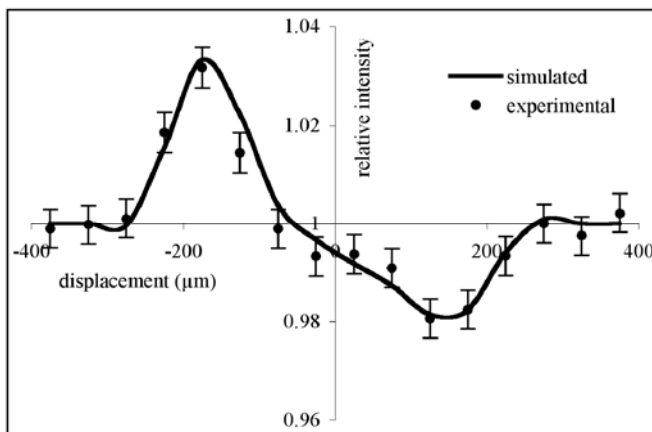


FIGURE 3. Measured x-ray profile of a thin wire showing peaks arising from phase contrast at both edges of the wire along with the simulated profile (solid line)

ACKNOWLEDGMENTS

This work was supported by the Wellcome Trust (085856/Z/08/Z). A. Olivo is supported by a Career Acceleration Fellowship awarded by the UK Engineering and Physical Sciences Research Council (EP/G004250/1).

REFERENCES

1. A. W. Stevenson et al., *Nucl. Instrum. Methods B* **199**, 427 (2003).
2. M. A. Simon et al., *Curr. Biol.* **20**, 1458 (2010).
3. A. Snigirev, I. Snigireva, V. Kohn, S. Kuznetsov, and I. Schelokov, *Rev. Sci. Instrum.* **66**, 5486 (1995).
4. D. Chapman et al., *Phys. Med. Biol.* **42**, 2015 (1997).
5. A. Momose, *Nucl. Instr. Meth. A* **352**, 622 (1995).
6. P. Cloetens et al., *Appl. Phys. Lett.* **75**, 2912 (1999).
7. E. Castelli et al., *Nucl. Instrum. Methods A* **572**, 237 (2007).
8. S. W. Wilkins, T. E. Gureyev, D. Gao, A. Pogany, A.W. Stevenson, *Nature* **384**, 335 (1996).
9. F. Pfeiffer, T. Weitkamp, O. Bunk, and C. David, *Nature Physics* **2**, 258 (2006).
10. A. Momose, W. Yashiro, H. Kuwabara, and K. Kawabata, *Jpn. J. Appl. Phys.* **48**, 076512 (2009).
11. A. Olivo and R. Speller, *Appl. Phys. Lett.* **91**, 074106 (2007).
12. A. Olivo and R. Speller, *Phys. Med. Biol.* **52**, 6555 (2007).